Z. Phys. C – Particles and Fields 48, 543–551 (1990)

Zeitschrift für Physik C Particles and Fields

Exclusive hadronic decays of *B* mesons

ARGUS Collaboration

H. Albrecht, H. Ehrlichmann, G. Harder, A. Krüger, A. Nau, A.W. Nilsson, A. Nippe, T. Oest, M. Reidenbach, M. Schäfer, W. Schmidt-Parzefall, H. Schröder, H.D. Schulz, F. Sefkow, R. Wurth
DESY, D-2000 Hamburg, Federal Republic of Germany

R.D. Appuhn, A. Drescher, C. Hast, G. Herrera, H. Kolanoski, A. Lange, A. Lindner, R. Mankel, H. Scheck, M. Schieber, G. Schweda, B. Spaan, A. Walther, D. Wegener
Institut für Physik[1], Universität Dortmund, D-4600 Dortmund, Federal Republic of Germany

M. Paulini, K. Reim, U. Volland, H. Wegener
Physikalisches Institut[2], Universität Erlangen-Nürnberg, D-8520 Erlangen, Federal Republic of Germany

W. Funk, J. Stiewe, S. Werner
Institut für Hochenergiephysik[3], Universität Heidelberg, D-6900 Heidelberg, Federal Republic of Germany

S. Ball, J.C. Gabriel, C. Geyer, A. Hölscher, W. Hofmann, B. Holzer, S. Khan, J. Spengler
Max Planck-Institut für Kernphysik, D-6900 Heidelberg, Federal Republic of Germany

D.I. Britton[4], C.E.K. Charlesworth[5], K.W. Edwards[6], H. Kapitza[6], P. Krieger[5], R. Kutschke[5], D.B. MacFarlane[4], K.W. McLean[4], R.S. Orr[5], J.A. Parsons[5], P.M. Patel[4], J.D. Prentice[5], S.C. Seidel[5], G. Tsipolitis[4], K. Tzamariudaki[4], T.-S. Yoon[5]
Institute of Particle Physics[7], Canada

T. Ruf[8], S. Schael, K.R. Schubert, K. Strahl, R. Waldi, S. Weseler
Institut für Experimentelle Kernphysik[9], Universität Karlsruhe, D-7500 Karlsruhe, Federal Republic of Germany

B. Boštjančič, G. Kernel, P. Križan[10], E. Križnič, T. Živko
Institut J. Stefan and Oddelek za fiziko[11], Univerza v Ljubljani, Ljubljana, Yugoslavia

H.I. Cronström, L. Jönsson
Institute of Physics[12], University of Lund, Sweden

A. Babaev, M. Danilov, A. Droutskoy, B. Fominykh, A. Golutvin, I. Gorelov, F. Ratnikov, V. Lubimov, A. Rostovtsev, A. Semenov, S. Semenov, V. Shevchenko, V. Soloshenko, V. Tchistilin, I. Tichomirov, Yu. Zaitsev
Institute of Theoretical and Experimental Physics, Moscow, USSR

R. Childers, C.W. Darden
University of South Carolina[13], Columbia, SC, USA

Received 16 May 1990

[1] Supported by the German Bundesministerium für Forschung und Technologie, under contract number 054DO51P
[2] Supported by the German Bundesministerium für Forschung und Technologie, under contract number 054ER12P
[3] Supported by the German Bundesministerium für Forschung und Technologie, under contract number 054HD24P
[4] McGill University, Montreal, Quebec, Canada
[5] University of Toronto, Toronto, Ontario, Canada
[6] Carleton University, Ottawa, Ontario, Canada
[7] Supported by the Natural Sciences and Engineering Research Council, Canada
[8] Now at ETH Zürich, Switzerland
[9] Supported by the German Bundesministerium für Forschung und Technologie, under contract number 054KA17P
[10] Supported by Alexander v. Humboldt Stiftung, Bonn
[11] Supported by Raziskovalna skupnost Slovenije and the Internationales Büro KfA, Jülich
[12] Supported by the Swedish Research Council
[13] Supported by the U.S. Department of Energy, under contract DE-AS09-80ER10690

Abstract. Using the ARGUS detector at the e^+e^- storage ring DORIS II, we have measured B decays into exclusive final states containing a D or D^* meson plus several pions, or containing a J/ψ or ψ' meson plus a strange particle. Some of these channels have not been seen before, while others represent updated measurements of previous results. The branching ratios are compared with the predictions of the model of Bauer, Stech and Wirbel. Using the cleanest decay channels, the mass of the charged and neutral B meson are found to be $m_{B^-}=(5280.5\pm1.0\pm2.0)\,\mathrm{MeV/c^2}$ and $m_{B^0}=(5279.6\pm0.7\pm2.0)\,\mathrm{MeV/c^2}$ respectively, yielding a mass difference $m_{B^0}-m_{B^-}=(-0.9\pm1.2\pm0.5)\,\mathrm{MeV/c^2}$.

1 Introduction

Measurements of exclusive B meson decay rates allow for tests of theoretical models of the weak decays of heavy quarks. Due to the large mass of the b quark, the influence of the strong interaction can be calculated more reliably than for the decays of lighter mesons. There are several models available which describe hadronic B decays [1–5]. In addition, reconstruction in hadronic channels provides the only means of determining the B^0 and B^+ masses. A measurement of their mass splitting is a test of the quark model predictions, and an essential input to estimates of the ratio of charged-to-neutral production on the $\Upsilon(4S)$.

This paper summarizes ARGUS measurements of exclusive hadronic B decays involving $b\to c$ transitions. B mesons are produced through the reaction $e^+e^-\to\Upsilon(4S)\to B\bar{B}$ and are reconstructed in hadronic decay modes with multiparticle final states. In particular, channels with a D, D^*, J/ψ or ψ' meson have been studied. The measurement of branching ratios for two-body B decays involving a J/ψ or ψ' meson are of wide interest in the light of proposals for the study of CP violation in future experiments. Results are reported for previously unseen B decay channels, along with updated measurements for other modes [6–8].

2 Data analysis

The data used in this analysis are collected with the ARGUS detector at the e^+e^- storage ring DORIS II at DESY. An integrated luminosity of 229 $\mathrm{pb^{-1}}$ has been collected on the $\Upsilon(4S)$ resonance which corresponds to about 192,000 $\Upsilon(4S)$ decays. The ARGUS detector is a 4π magnetic spectrometer described in detail elsewhere [9]. Charged hadrons are identified on the basis of specific ionization in the drift chamber (dE/dx) and time of flight (TOF) measurements. For all charged tracks, a likelihood ratio for each of the particle hypotheses e, μ, π, K and p is calculated. All hadron hypotheses with a likelihood ratio greater than 1% are accepted. For lepton identification, information from the electromagnetic calorimeter and muon chamber is used, in addition to the dE/dx and TOF measurements.

The geometrical acceptance of the data sample is defined by restricting the polar angle θ of hadrons with respect to the beam line to the region $|\cos\theta|<0.92$. Furthermore, charged particles are required to have a momentum larger than 60 MeV/c, and photons an energy larger than 50 MeV.

In order to suppress the background contribution from continuum and QED events, low multiplicity events are rejected by the requirement $n_{\mathrm{ch}}+n_\gamma/2\geqq5$, where n_γ is the number of photons with energy larger than 100 MeV, and n_{ch} is the number of charged tracks. In addition, the event is rejected, if the momentum of any charged particle in the event exceeds 3 GeV/c.

Leptons, used for the reconstruction of J/ψ and ψ' mesons, are required to have momenta greater than 900 MeV/c, K^0_S mesons are reconstructed from $\pi^+\pi^-$ combinations forming a secondary vertex. The invariant mass of the pair is required to fit the K^0_S mass hypothesis with a χ^2 less than 16. All combinations of two photons satisfying the π^0 mass hypothesis with a χ^2 less than 6 are accepted as π^0 candidates. High-energy π^0's, whose decay photons may merge into a single cluster in the calorimeter, are included in the sample by considering all clusters with energy greater than 800 MeV as π^0 candidates.

3 B decays into D and D^* mesons

Measurements of inclusive D meson rates on the $\Upsilon(4S)$ resonance show that the majority of B decays produce D mesons [10–12], as expected from the dominance of $b\to c$ transitions. The momentum spectra of the D and D^* mesons are found to be soft, reflecting a substantial multibody component in hadronic decays. Therefore, we have studied the exclusive decays of B mesons into a D or D^* meson plus up to four pions. The specific channels examined are*:

$$
\begin{array}{ll}
B^-\to D^0\pi^-, & \bar{B}^0\to D^+\pi^-,\\
B^-\to D^0\pi^-\pi^0(\rho^-), & \bar{B}^0\to D^+\pi^-\pi^0(\rho^-),\\
B^-\to D^{*0}\pi^-, & \bar{B}^0\to D^{*+}\pi^-,\\
B^-\to D^{*0}\pi^-\pi^0(\rho^-), & \bar{B}^0\to D^{*+}\pi^-\pi^0(\rho^-),\\
B^-\to D^{*+}\pi^-\pi^-, & \bar{B}^0\to D^{*+}\pi^-\pi^-\pi^+,\\
B^-\to D^{*+}\pi^-\pi^-\pi^0, & \bar{B}^0\to D^{*+}\pi^-\pi^-\pi^+\pi^0,\\
B^-\to D^{*+}\pi^-\pi^-\pi^-\pi^+, &
\end{array}
$$

where the D^* and D mesons are reconstructed in the following channels:

$$
\begin{array}{l}
D^{*+}\to D^0\pi^+,\\
D^{*0}\to D^0\pi^0,
\end{array}
$$

$$
\begin{array}{ll}
D^0\to K^-\pi^+, & D^+\to K^0_S\pi^+,\\
D^0\to K^0_S\pi^+\pi^-, & D^+\to K^-\pi^+\pi^+,\\
D^0\to K^-\pi^+\pi^-\pi^+, & D^+\to K^0_S\pi^+\pi^+\pi^-,\\
D^0\to K^-\pi^+\pi^0. &
\end{array}
$$

* References in this paper to a specific charged state imply the charged conjugate state also

All D^0, D^+, D^{*+}, and D^{*0} candidates are required to be consistent with the appropriate mass hypothesis with a χ^2 of less than 6. In addition, the candidates are required to have a mass lying within a restricted interval around the nominal value. The allowed ranges are chosen to be ± 3 MeV/c^2 for the D^{*+}, ± 15 MeV/c^2 for the D^{*0} and ± 30 to 40 MeV/c^2 for the D^0 and D^+ mesons. The channel $D^0 \to K^- \pi^+ \pi^0$ suffers from a large combinatorial background, and hence is only used for reconstructing the modes $\bar{B}^0 \to D^{*+} \pi^-$ and $B^- \to D^{*+} \pi^- \pi^-$, where the B signal is particularly clean. The requirement of a D^{*+}, detected via its decay into $D^0 \pi^+$, results in a large reduction of the combinatorial background, because of the excellent mass resolution for the D^{*+} (1.0 MeV/c^2) brought about by the low Q value for the decay. Momentum resolution is generally improved by application of mass constraint fits to all intermediate states, where the natural width is smaller than the detector resolution (K^0_S, π^0, D^0, D^+, D^{*0}, and D^{*+}).

In the search for B candidates, two global requirements are made on all $Dn\pi$ and $D^*n\pi$ combinations:

- The energy of the candidate must be close to the beam energy. The experimental energy resolution σ_E of these combinations varies between 20 to 30 MeV for the charged channels, 30 to 50 MeV for channels involving a π^0 reconstructed from two photons, to over 100 MeV for channels where only one cluster is required for the π^0. We require $|E - E_{\text{beam}}| < 2\sigma_E$ for the $D^{*+} 4\pi$ and (D^+, D^0 or D^{*0}) $n\pi$ decay modes, and apply a $3\sigma_E$ cut for all others.
- The total probability for the candidate, calculated from the sum of all χ^2 contributions from particle identification and kinematic fits, must exceed 1%.

Additional requirements are made for specific channels only:

- In order to suppress continuum events, a cut is made on the angle α between the thrust axis of the B candidate and the thrust axis of the remainder of the event. This distribution should be almost isotropic for $\Upsilon(4S)$ decays, whereas for continuum events it is strongly peaked at $|\cos\alpha| = 1$. We require $|\cos\alpha| < 0.7$ for the decay channels $B \to (D^+, D^0$ or $D^{*0}) n\pi$ and $|\cos\alpha| < 0.8$ for the decay $\bar{B}^0 \to D^{*+} \pi^-$.
- In the decay $B \to D\rho$, the ρ is produced with helicity 0, yielding a $\cos^2\theta_\pi$ distribution for the angle θ_π between one of the pions from the ρ decay and the helicity axis in the ρ rest frame. Therefore we restricted this angle to the interval $|\cos\theta_\pi| > 0.5$. In addition, the $\pi^- \pi^0$ mass is required to lie within ± 150 MeV/c^2 of the ρ mass.
- For the $D^{*+} n\pi$ combinations we require that all particle subcombinations have a momentum smaller than 2.5 GeV/c. For $D^{*+} 4\pi$ combinations, the $D^0 \pi^+$ combinations are required to have a mass value lying ± 1 MeV/c^2 around the nominal D^{*+} mass.

A kinematic fit is then applied to all accepted B meson candidate constraining their energy to the beam energy. This improves the moderate mass resolution by roughly one order of magnitude to about 4.0 to 4.5 MeV/c^2 for combinations in the B mass region, depending slightly on the B decay channel.

All combinations with a mass greater than 5.17 GeV/c^2 are considered as B candidates. There are events with more than one candidate per event in the same B decay channel, especially in the channels with π^0's were the combinatorial background is high. Only one candidate per decay channel and per event is accepted, by choosing the candidate with the highest total probability calculated for the sum of all χ^2 contributions from particle identification, kinematical fits and the beam energy constraint fit.

3.1 Fitting procedure and branching ratio determinations

Figure 1 shows the combined B signal in the $D^{*+} n\pi (n \leqq 3)$ decay channels. A check has been made that the analysis procedure does not bias the mass distribution. For this check, wrong-charge combinations have been used, i.e., combinations where the charge of one pion differs from the charge of the corresponding particle in the analysed candidate channels. As can be seen from the hatched histogram, the mass distribution of wrong-charge combinations, normalized in the region below 5.25 GeV/c^2, provides an excellent description of the background shape in the spectrum of B candidates. The shape of the background can be parameterized by the function

$$\frac{dN}{dM} = aM \sqrt{1 - \frac{M^2}{E^2_{\text{beam}}}} \cdot \exp\left(-b\left(1 - \frac{M^2}{E^2_{\text{beam}}}\right)\right),$$

where a and b are free parameters. The first term describes the threshold behaviour, while the exponential factor is an empirical model of the drop in the background toward smaller masses. This function describes perfectly the background in the right charge distribution for masses smaller than the B mass. It is also in good agreement with the wrong-charge distribution and furthermore supported by Monte Carlo studies.

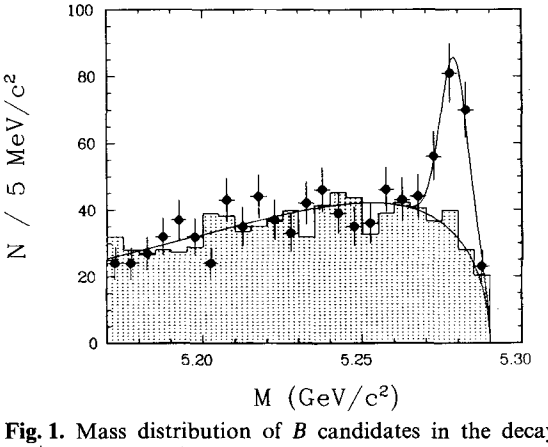

Fig. 1. Mass distribution of B candidates in the decay channels $D^{*+} n\pi$ ($n \leqq 3$). The hatched area shows the same spectrum for wrong-charge combinations

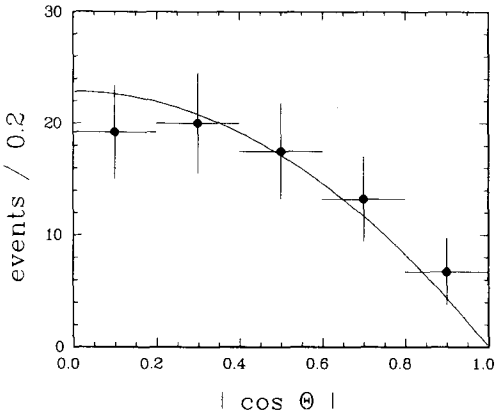

Fig. 2. Distribution of $|\cos\theta|$ for B candidates in clean two-body decay modes, as described in Fig. 9 below. The background is subtracted using the combinations in a mass sideband below the position of the B meson. The curve is a fit using a $\sin^2\theta$ distribution

The $\Upsilon(4S)$ resonance is a $J^P = 1^-$ state which is produced transversely polarized. Therefore a $\sin^2\theta$ distribution is expected for the production angle θ of the B mesons with respect to the beam direction. The observed distribution of $\cos\theta$ is shown in Fig. 2. The background has been subtracted using a sideband below the B signal. Only candidates from the clean two-body decay modes have been included in the plot.

Figure 3 shows the B signals of all channels containing a D or D^* meson. The two-body decay modes with only charged particles in the final state are relatively clean, in contrast to the much larger background for decay modes with π^0's or multiparticle final states.

Reconstruction efficiencies have been determined using simulated $\Upsilon(4S)$ decays. B decays into D and D^* mesons and several pions are uniformly generated in phase space. Where appropriate, two-body decays of B to $D\rho$ or $D^*\rho$ are also used. These events are passed through a detailed detector Monte Carlo and the ARGUS reconstruction program. The branching ratios of the D and D^* mesons are taken from [13] and [14], respectively, where $\mathrm{BR}(D^0 \to K^-\pi^+)$ and $\mathrm{BR}(D^{*+} \to D^0\pi^+)$ are reported to be $(4.2\pm0.6)\%$ and $(57\pm6)\%$ respectively. Since the mass difference is found to be zero within the experimental uncertainty (see Sect. 5), the charged and neutral B mesons are assumed to be produced at equal rates in $\Upsilon(4S)$ decays. Decays of the $\Upsilon(4S)$ to non-$B\bar{B}$ states are assumed negligible.

The resulting branching ratios for charged and neutral B mesons are shown in Table 1 and Table 2, respectively. The systematic errors quoted include uncertainties in the number of B mesons produced, in the D and D^* branching ratios, as well as in the shape of the background function and the determination of the efficiencies [15].

As a consistency check the analysis is repeated using tighter cuts on the measured B candidate energy. If the allowed interval is reduced to $\pm\sigma_E$ or to a fixed ± 40 MeV around the beam energy, the branching ratios obtained are found to be in good agreement with those given in Tables 1 and 2. Monte Carlo studies show that the energy constraint is sufficient to suppress contributions from other decay channels, where one particle is missed or exchanged. Therefre we conclude that conceivable correlated backgrounds are negligible.

Table 1. B^- decay modes

B decay	Signal events	Branching ratio
$B^- \to D^0\pi^-$	12 ± 5	$(0.20\pm0.08\pm0.06)\%$
$B^- \to D^0\rho^-$	19 ± 6	$(1.3\ \pm0.4\ \pm0.4)\%$
$B^- \to D^{*0}\pi^-$	9 ± 3	$(0.40\pm0.14\pm0.12)\%$
$B^- \to D^{*0}\rho^-$	7 ± 4	$(1.0\ \pm0.6\ \pm0.4)\%$
$B^- \to D^{*+}\pi^-\pi^-$	11 ± 6	$(0.26\pm0.14\pm0.07)\%$
$B^- \to D_J^{(*)0}\pi^-$	6 ± 3	see text
$B^- \to D^{*+}\pi^-\pi^-\pi^0$	26 ± 10	$(1.8\ \pm0.7\ \pm0.5)\%$
$B^- \to D_J^{(*)0}\rho^-$	5 ± 3	see text
$B^- \to D^{*+}\pi^-\pi^-\pi^-\pi^+$	<9	$<1.0\%$ at 90% C.L.
$B^- \to J/\psi K^-$	6	$(0.07\pm0.03\pm0.01)\%$
$B^- \to \psi' K^-$	5	$(0.18\pm0.08\pm0.04)\%$
$B^- \to J/\psi K^{*-}$	2	$(0.16\pm0.11\pm0.03)\%$
$B^- \to \psi' K^{*-}$	<3.9	$<0.49\%$ at 90% C.L.
$B^- \to J/\psi K^-\pi^+\pi^-$	<8	$<0.16\%$ at 90% C.L.
$B^- \to \psi' K^-\pi^+\pi^-$	3	$(0.19\pm0.11\pm0.04)\%$

Table 2. $\bar{B}^0$ decay modes

B decay	Signal events	Branching ratio
$\bar{B}^0 \to D^+\pi^-$	$22\pm\ 5$	$(0.48\pm0.11\pm0.11)\%$
$\bar{B}^0 \to D^+\rho^-$	$9\pm\ 5$	$(0.9\pm0.5\pm0.3)\%$
$\bar{B}^0 \to D^{*+}\pi^-$	$12\pm\ 4$	$(0.28\pm0.09\pm0.06)\%$
$\bar{B}^0 \to D^{*+}\pi^-\pi^0$	51 ± 10	$(1.8\pm0.4\pm0.5)\%$
$\bar{B}^0 \to D^{*+}\rho^-$	$19\pm\ 9$	$(0.7\pm0.3\pm0.3)\%$
$\bar{B}^0 \to D^{*+}\pi^-\pi^-\pi^+$	$26\pm\ 7$	$(1.2\pm0.3\pm0.4)\%$
$\bar{B}^0 \to D^{*+}\pi^-\pi^-\pi^+\pi^0$	28 ± 10	$(4.1\pm1.5\pm1.6)\%$
$\bar{B}^0 \to J/\psi K_S^0$	2	$(0.04\pm0.03\pm0.01)\%$
$\bar{B}^0 \to \psi' K_S^0$	<2.3	$<0.14\%$ at 90% C.L.
$\bar{B}^0 \to J/\psi \bar{K}^{*0}$	6	$(0.11\pm0.05\pm0.02)\%$
$\bar{B}^0 \to \psi' \bar{K}^{*0}$	<3.9	$<0.23\%$ at 90% C.L.
$\bar{B}^0 \to \psi' K^-\pi^+$	<2.3	$<0.10\%$ at 90% C.L.

Several decay modes are observed for the first time. The $D^{*0}\pi^-$ invariant mass distribution is shown in Fig. 3e, where a mass constraint fit is performed on the $D^0\pi^0$ intermediate state. A demonstration that the $D^0\pi^0$ actually forms a D^{*0} can be seen in Fig. 4, where $D^0\pi^0$ combinations from candidates for the decay $B^- \to D^0\pi^0\pi^-$ with mass greater than $5.27\,\mathrm{GeV/c^2}$ are shown, without the mass constraint fit on the $D^0\pi^0$ subsystem. At the $D^0\pi^0$ threshold evidence for a signal of (6 ± 3) events is visible. The fitted mass agrees with the nominal value for the D^{*0} [16]. In the decay channel $\bar{B}^0 \to D^{*+}\pi^-\pi^-\pi^+\pi^0$, shown in Fig. 3l, a signal is seen above a relatively large background. No evidence for the decay $B^- \to D^{*+}\pi^-\pi^-\pi^-\pi^+$ is found.

3.2 Resonant decomposition

In the final states with several pions we search for resonant subsystems. Figure 5 shows the combined $\pi^-\pi^0$ in-

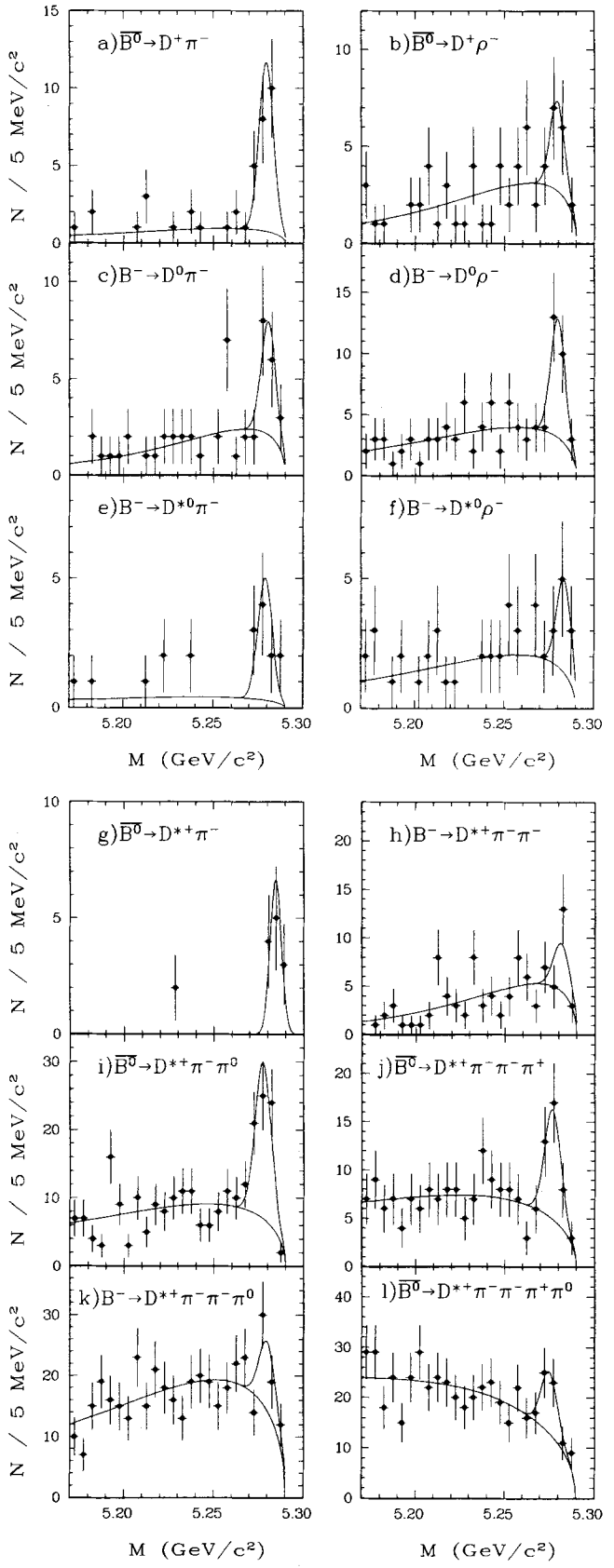

Fig. 3a–l. Separate mass distributions for decay channels containing a D and D^*: **a** $\bar{B}^0 \to D^+\pi^-$, **b** $\bar{B}^0 \to D^+\rho^-$, **c** $B^- \to D^0\pi^-$, **d** $B^- \to D^0\rho^-$, **e** $B^- \to D^{*0}\pi^-$, **f** $B^- \to D^{*0}\rho^-$, **g** $\bar{B}^0 \to D^{*+}\pi^-$, **h** $B^- \to D^{*+}\pi^-\pi^-$, **i** $\bar{B}^0 \to D^{*+}\pi^-\pi^0$, **j** $\bar{B}^0 \to D^{*+}\pi^-\pi^-\pi^+$, **k** $B^- \to D^{*+}\pi^-\pi^-\pi^0$, **l** $\bar{B}^0 \to D^{*+}\pi^-\pi^-\pi^+\pi^0$

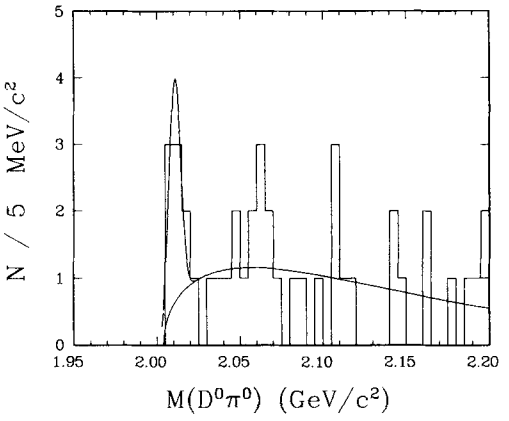

Fig. 4. Mass distribution of $D^0\pi^0$ in the decay $B^- \to D^0\pi^0\pi^-$

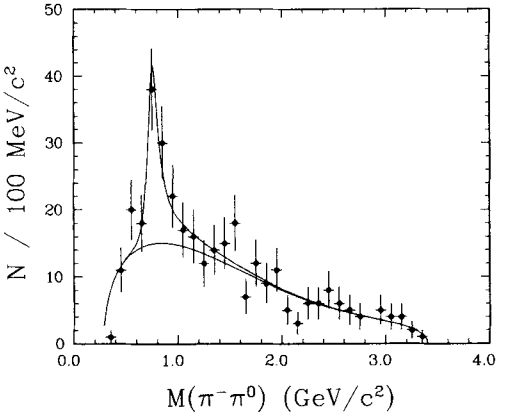

Fig. 5. Mass distribution of $\pi^-\pi^0$ for the decays $\bar{B}^0 \to D^{*+}\pi^-\pi^0$, $B^- \to D^{*0}\pi^-\pi^0$, $\bar{B}^0 \to D^+\pi^-\pi^0$, and $B^- \to D^0\pi^-\pi^0$, for B candidates with mass greater than 5.270 GeV/c²

variant mass spectrum for B candidates with mass greater than 5.27 GeV/c² in the decay channels $\bar{B}^0 \to D^{*+}\pi^-\pi^0$, $B^- \to D^{*0}\pi^-\pi^0$, $\bar{B}^0 \to D^+\pi^-\pi^0$ and $B^- \to D^0\pi^-\pi^0$. Fitting the signal with a relativistic Breit-Wigner function for the ρ and a second-order polynomial multiplied by a threshold factor for the background, we obtain (57 ± 14) ρ candidates. In the B sideband below 5.27 GeV/c², no ρ signal is seen. After removal of the $D^{*0}\pi^-$ candidates from the $D^0\pi^-\pi^0$ data sample, the $D\pi^-\pi^0$ and $D^{*0}\pi^-\pi^0$ signals are found to be entirely consistent with $D\rho$ and $D^{*0}\rho$. Fitting the $\pi^-\pi^0$ invariant mass distribution of those events in the B mass region, we find (41 ± 11) events in these 3 channels. A fit of the B signal itself, after a 150 MeV/c² cut around the ρ, yields (35 ± 9) events. In the $D^{*+}\pi^-\pi^0$ channel, on the other hand, there is room for a significant non-ρ contribution.

In the $\bar{B}^0 \to D^{*+}\pi^-\pi^-\pi^+$ channel most of the signal is consistent with $D^{*+}\pi^-\rho^0$. In Fig. 6a the mass distribution for $\pi^-\pi^+$ combinations is displayed. A ρ peak is visible although the combinatorial background is large. Figure 6b shows the invariant mass spectrum of the $D^{*+}\pi^-\pi^-\pi^+$ combination with and without the requirement that at least one of the two $\pi^-\pi^+$ combinations has an invariant mass within 150 MeV/c² of the

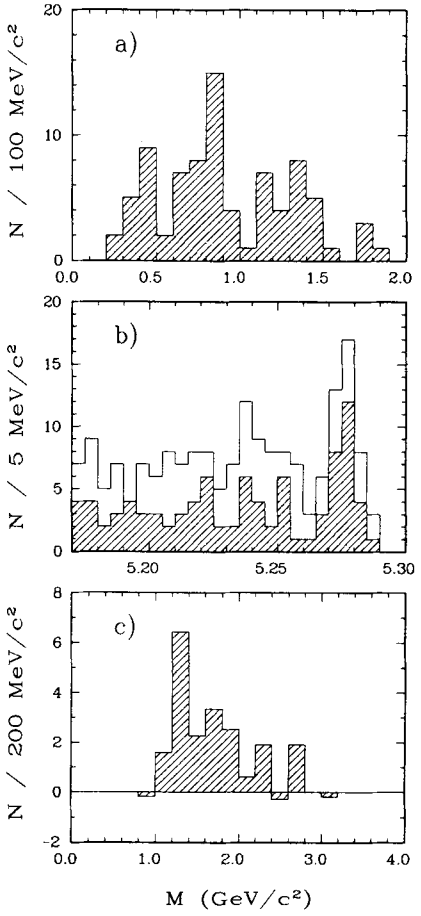

Fig. 6a–c. For the decay channel $\bar{B}^0 \to D^{*+}\pi^-\pi^-\pi^+$: **a** Mass distribution of $\pi^-\pi^+$ pairs for B candidates with mass greater than 5.270 GeV/c². The histogram contains 2 entries per event. **b** Mass distribution of $D^{*+}\pi^-\pi^-\pi^+$ combinations with (hatched area) or without (open histogram) a requirement that at least one $\pi^+\pi^-$ pair have a mass within ± 150 MeV/c² of the nominal value of the ρ mass. **c** Mass of the $\pi^-\pi^-\pi^+$ system after the ρ cut described in **b** for B candidates with mass greater than 5.27 GeV/c². The background is subtracted using the low-mass sideband to the B signal

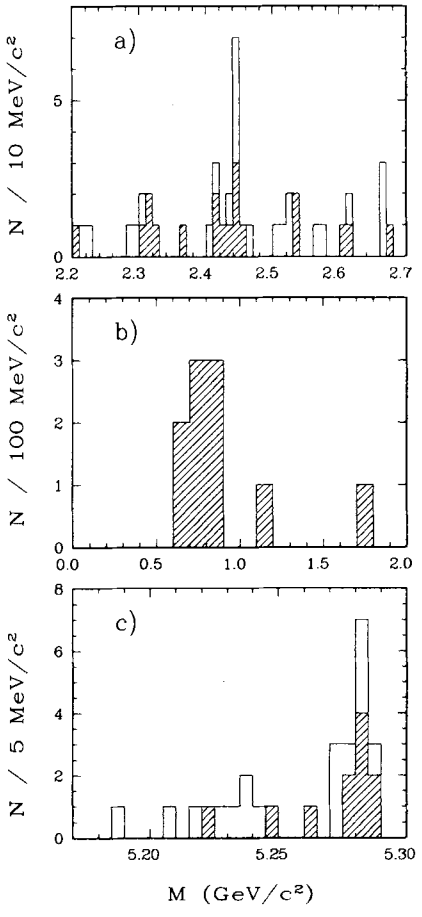

Fig. 7a–c. For the decay channels $B^- \to D^{*+}\pi^-\pi^-$ and $B^- \to D^{*+}\pi^-\pi^-\pi^0$: **a** Mass distribution of $D^{*+}\pi^-$ combinations in the decay channels $B^- \to D^{*+}\pi^-\pi^-$ and $B^- \to D^{*+}\pi^-\pi^-\pi^0$ (with the remaining $\pi^-\pi^0$ pair lies within ± 150 MeV/c² of the nominal ρ mass), for B candidates with a mass greater than 5.270 GeV/c². The hatched area shows the contribution from the $B^- \to D^{*+}\pi^-\pi^-$ decay channel alone. **b** Mass distribution of $\pi^-\pi^0$ combinations in the decay channel $B^- \to D^{*+}\pi^-\pi^-\pi^0$, with the $D^{*+}\pi^-$ invariant mass in the range from 2.4 to 2.47 GeV/c², for B candidates with mass greater than 5.27 GeV/c². **c** Mass distribution for B candidates after requiring the $D^{*+}\pi^-$ invariant mass lie between 2.4 and 2.47 GeV/c², a range which includes both $D_J^{(*)0}$ resonances. The decay channel $B^- \to D^{*+}\pi^-\pi^-\pi^0$ includes a cut on the ρ^- meson as described in the text. The hatched area shows the contribution from the decay channel $B^- \to D^{*+}\pi^-\pi^-$ alone

nominal ρ mass. The fitted number of events with the cut on the ρ mass is 20 ± 6, compared to 26 ± 7 without, while the background level drops by a factor of two. However, only part of the signal can be attributed to the $a_1(1260)$, based on Fig. 6c. Here the mass of the $\pi^-\pi^-\pi^+$ system, after requiring that the intermediate $\pi^-\pi^+$ mass lies in the ρ band, is shown. The background has been subtracted using the B signal mass sideband. Clearly the observed spectrum extends to 3π masses larger than expected for the $a_1(1260)$.

In the $B^- \to D^{*+}\pi^-\pi^-$ and $B^- \to D^{*+}\pi^-\pi^-\pi^0$ decay channels we find some evidence for the production of P-wave D mesons, as demonstrated in Fig. 7a. The $D^{*+}\pi^-$ mass distribution of these channels peaks between 2.4 and 2.5 GeV/c². For the channel $B^- \to D^{*+}\pi^-\pi^-\pi^0$, the invariant mass of the π^0 and the bachelor π^- is restricted to lie within ± 150 MeV/c² of the ρ mass. In this $D^{*+}\pi^-$ mass region are two overlapping resonances, as recently reported [17–20]. One is the $D_1^0(2414)$, a $J^P = 1^+$ state (mass $= 2414 \pm 2 \pm 5$ MeV/c², $\Gamma = 13 \pm 6^{+10}_{-5}$ MeV/c² [19]) and the other is the $D_2^{*0}(2459)$, which is a 2^+ meson (mass $= 2455 \pm 3 \pm 5$ MeV/c², $\Gamma = 15^{+13}_{-10} \pm 5_{10}$ MeV/c² [18]). Due to low statistics and the large uncertainties on the widths, the separate contributions from the two states cannot be distinguished. In the following we refer to resonant $D^{*+}\pi^-$ combinations as $D_J^{(*)0}$. Fitting the mass distribution with the nominal values of the two resonances we obtain (6 ± 3) events in the $B^- \to D^{*+}\pi^-\pi^-$ and (5 ± 3) events in the $B^- \to D^{*+}\pi^-\pi^-\pi^0$ decay channel above a flat background. A cut on the $D^{*+}\pi^-$ mass from 2.4 to 2.47 GeV/c², which includes both resonances, gives

a clean ρ signal in the $B^- \to D^{*+}\pi^-\pi^-\pi^0$ channel (Fig. 7b). This also demonstrates that there is no large $D_J^{(*)0}\pi^-\pi^0$ contribution with nonresonant $\pi^-\pi^0$ states. After a cut on the $D_J^{(*)0}$ intermediate state a clean B signal is seen in both channels (Fig. 7c). From this we can determine the branching ratios:

$$\mathrm{BR}(B^- \to D_J^{(*)0}\pi^-) \times \mathrm{BR}(D_J^{(*)0} \to D^{*+}\pi^-) = (0.14 \pm 0.07 \pm 0.04)\%,$$

$$\mathrm{BR}(B^- \to D_J^{(*)0}\rho^-) \times \mathrm{BR}(D_J^{(*)0} \to D^{*+}\pi^-) = (0.35 \pm 0.21 \pm 0.10)\%.$$

4 B decays into J/ψ and ψ' mesons

The momentum spectrum of J/ψ mesons from B decays is soft [7, 11], indicating a substantial multibody component as in the case of B decays involving a D or D^* meson. The two-body B decays involving a J/ψ or ψ' are observable despite their small branching ratios, because they are nearly free of background and the reconstruction efficiencies are high, compared to those for D and D^* decays. The analysis of multi-body decay modes, on the other hand, encounters background problems. Hence the following decay modes have been studied:

$B^- \to J/\psi K^-$,	$\bar{B}^0 \to J/\psi K_S^0$,
$B^- \to \psi' K^-$,	$\bar{B}^0 \to \psi' K_S^0$,
$B^- \to J/\psi K^{*-}$,	$\bar{B}^0 \to J/\psi \bar{K}^{*0}$,
$B^- \to \psi' K^{*-}$,	$\bar{B}^0 \to \psi' \bar{K}^{*0}$,
$B^- \to J/\psi K^-\pi^+\pi^-$,	$\bar{B}^0 \to J/\psi K^-\pi^+$,
$B^- \to \psi' K^-\pi^+\pi^-$,	$\bar{B}^0 \to \psi' K^-\pi^+$.

The J/ψ mesons are reconstructed in their leptonic decay modes. For the e^+e^- decay mode an asymmetric cut of $+100\,\mathrm{MeV/c^2}$ and $-200\,\mathrm{MeV/c^2}$ around the nominal J/ψ mass is used in order to account for the radiative tail, while for the $\mu^+\mu^-$ mode a symmetric cut of $\pm 100\,\mathrm{MeV/c^2}$ and a χ^2 cut of 9 around the nominal J/ψ mass is used. The ψ' is reconstructed in its leptonic decay modes as well as in the decay mode $\psi' \to J/\psi\pi^+\pi^-$. The invariant mass of ψ' candidates is required to be consistent with the nominal ψ' mass with a χ^2 of less than 9, and to lie within $\pm 100\,\mathrm{MeV/c^2}$ for the leptonic modes and within $\pm 10\,\mathrm{MeV/c^2}$ for the $J/\psi\pi^+\pi^-$ mode. A mass constraint fit is then performed on both charmonium mesons. The K^* mesons are reconstructed through both isospin combinations of $K\pi$, except for the $B^- \to J/\psi K^{*-}$ decay channel where only the $K_S^0\pi^-$ mode is used for the K^{*-} reconstruction. All $K\pi$ combinations whose invariant mass is within $\pm 100\,\mathrm{MeV/c^2}$ of the nominal K^* mass are taken as K^* candidates. The subsequent reconstruction of exclusive B decays then proceeds as described in Sect. 3.

Figure 8 shows the invariant mass distribution of those channels where a positive signal is seen, as well as several channels without a signal. The number of signal events in the clean decay modes, like the two-body decay modes, is determined by counting the number of

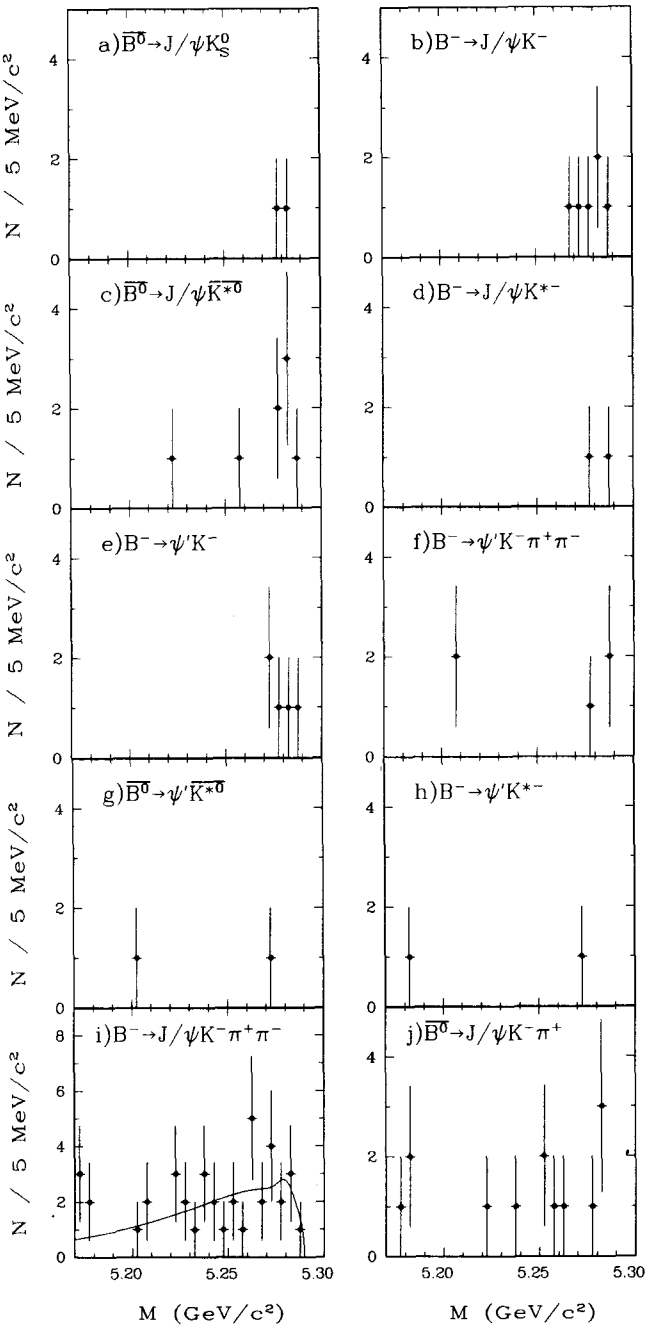

Fig. 8a–j. Mass distributions for J/ψ and ψ' decay channels: **a** $\bar{B}^0 \to J/\psi K_S^0$, **b** $B^- \to J/\psi K^-$, **c** $\bar{B}^0 \to J/\psi \bar{K}^{*0}$, **d** $B^- \to J/\psi K^{*-}$, **e** $B^- \to \psi' K^-$, **f** $B^- \to \psi' K^-\pi^+\pi^-$, **g** $\bar{B}^0 \to \psi' \bar{K}^{*0}$, **h** $B^- \to \psi' K^{*-}$, **i** $B^- \to J/\psi K^-\pi^+\pi^-$, **j** $\bar{B}^0 \to J/\psi K^-\pi^+$

events in the signal region 5.265 to $5.290\,\mathrm{GeV/c^2}$. For the other decay modes a fit is done with a gaussian for the signal and the background function given in Sect. 3.1. The branching ratios for the charged and neutral B mesons are shown in Table 1 and 2, respectively. The 3-body decay $\bar{B}^0 \to J/\psi K^-\pi^+$ is found to be consistent with $\bar{B}^0 \to J/\psi \bar{K}^{*0}$. The sum of the measured exclusive two-body J/ψ branching ratios is $(0.21 \pm 0.07 \pm 0.02)\%$, which is about 20% of the inclusive rate. This accounts for most of the hard component ($p > 1.4\,\mathrm{GeV/c}$) of the J/ψ momentum spectrum.

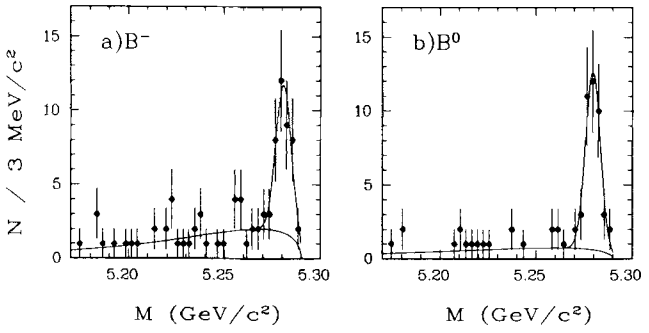

Fig. 9a, b. Mass distribution for B candidates in clean two-body channels: **a** B^- candidates from the channels: $B^- \to D^0\pi^-$, $D^{*0}\pi^-$, $D_J^{(*)0}\pi^-$, $J/\psi(K^-, K^{*-})$, and $\psi' K^-$, **b** $\bar{B}^0$ candidates from the channels: $\bar{B}^0 \to D^+\pi^-$, $D^{*+}\pi^-$, and $J/\psi(K_S^0, K^{*0})$

5 Masses of the charged and neutral B mesons

In order to minimize systematic uncertainties due to the influence of background, only clean decay channels, i.e., the two-body decay modes, are used for the determination of the masses of the neutral and charged B mesons. The mass distributions of the charged and neutral B meson candidates are shown in Fig. 9a and 9b, respectively. The fit gives the following results:

$$m_{B^0} = (5279.6 \pm 0.7 \pm 2.0)\ \mathrm{MeV/c^2},$$
$$m_{B^-} = (5280.5 \pm 1.0 \pm 2.0)\ \mathrm{MeV/c^2}.$$

The mass values are obtained using an energy scale defined by fixing the mass of the $\Upsilon(4S)$ to 10580 MeV/c^2 [16]. The systematic error includes the uncertainty on the mass of the $\Upsilon(4S)$ resonance (± 3.5 MeV/c^2), as well as uncertainties in the determination of the beam energy (± 1.0 MeV/c^2). The mass difference of the neutral and charged B meson is found to be:

$$m_{B^0} - m_{B^-} = (-0.9 \pm 1.2 \pm 0.5)\ \mathrm{MeV/c^2}.$$

The systematic error is derived by studying the influence of different assumptions for the shape of the background and varying the width of the B signals with the allowed uncertainty.

6 Discussion of the results

The large number of observed exclusive decay modes represents the most comprehensive list of ARGUS hadronic B decay measurements. Some interesting observations can be made regarding global properties of two-body decays involving a D or D^* plus a π or ρ in the final state. Assuming that the ratios of vector-to-pseudoscalar production are independent of the B meson charge, the following averages for the ratio of D^* to D production are obtained:

$$\mathrm{BR}(B \to D^*\pi)/\mathrm{BR}(B \to D\pi) = 1.0 \pm 0.3,$$
$$\mathrm{BR}(B \to D^*\rho)/\mathrm{BR}(B \to D\rho) = 0.8 \pm 0.4.$$

These results indicate that for two-body decays where the four-momentum squared of the off-shell W^- is small, corresponding to the mass of the π or ρ, the rate of D and D^* production is very similar. This is in marked contrast to inclusive D and D^* production [10, 11, 12], where approximately 75% of the inclusive D mesons originate from D^* decays. The other vector-to-pseudoscalar ratios:

$$\mathrm{BR}(B \to D\rho)/\mathrm{BR}(B \to D\pi) = 3.2 \pm 1.2,$$
$$\mathrm{BR}(B \to D^*\rho)/\mathrm{BR}(B \to D^*\pi) = 2.5 \pm 1.2,$$

show that there is a significant enhancement of ρ over π production. Altogether, only about 6% of the B^- and 9% of $\bar{B}^0$ decay modes have been observed through the exclusive hadronic modes investigated here, representing small fractions of the sum of the inclusive D^0 and D^+ meson branching ratios, $(70 \pm 11)\%$ [10].

The two-body decays can also be used to perform tests of theoretical models of weak decays. One model supplying a substantial list of exclusive B meson decays is that due to Bauer et al. [3]. Decays are grouped into three classes, which are described by parameters a_1, a_2 or a combination of both. Most modes are described by only one of the parameters, making it simple to determine their absolute value. For the extraction of results, the lifetime of the B meson is taken to be $\tau_B = (1.15 \pm 0.14) \cdot 10^{-12}$ s [10] and $V_{cb} = 0.045$ [21] is assumed.

The two-body $\bar{B}^0$ decays into D and D^* mesons are described by the a_1 parameter alone (Fig. 10a). Taking the four measured decay channels together we obtain $|a_1| = 1.02 \pm 0.11$. B meson decays into J/ψ mesons, on the other hand, are described only by the a_2 parameter (Fig. 10b). From all four decay channels taken together we find $|a_2| = 0.22 \pm 0.03$. The values of the two parameters determined from the individual channels are in agreement, supporting the universal description of two-body B decays with this model. The absolute ratio $|a_2/a_1|$ is 0.22 ± 0.04. The four two-body B^- decay modes into D or D^* mesons are described by an interference between the two amplitudes, allowing a determination of the rela-

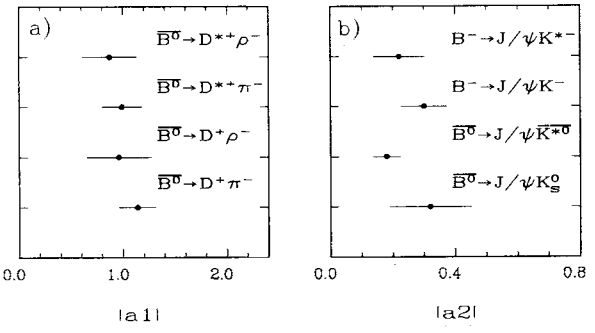

Fig. 10a, b. Determination of the parameters for the model of Bauer et al. [3]. The error bars represent the statistical and systematic uncertainties on the measured branching ratios added in quadrature. **a** Decay modes proportional to a_1: $\bar{B}^0 \to D^+\pi^-$, $D^+\rho^-$, $D^{*+}\pi^-$, and $D^{*+}\rho^-$, **b** Decay modes proportional to a_2: $\bar{B}^0 \to J/\psi K_S^0$, $J/\psi K^{*0}$, $B^- \to J/\psi K^-$, and $J/\psi K^{*-}$

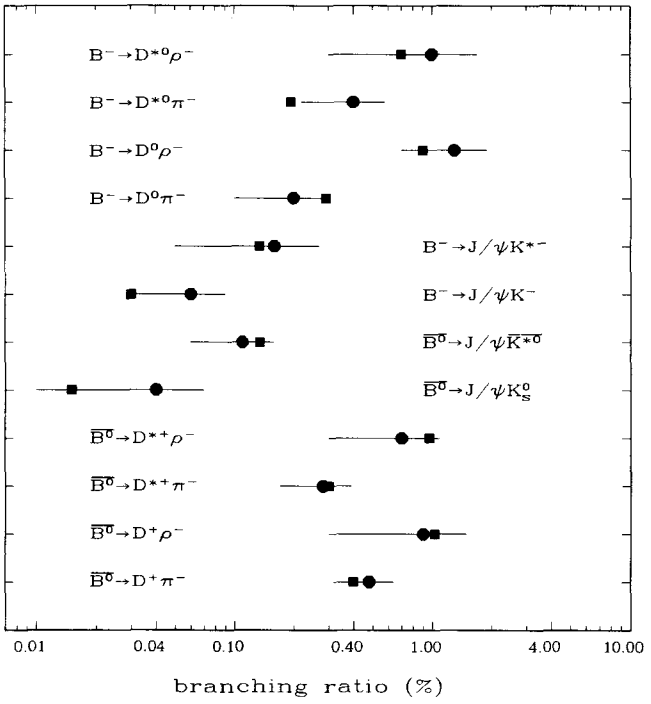

Fig. 11. Comparison between the experimentally measured branching ratios (solid points with errors combined statistical and systematic errors) and the prediction of the model of Bauer, Stech and Wirbel with $a_1 = 1.03$ and $a_2 = -0.20$

tive sign between the two parameters. Given the sizeable uncertainty on the ratio and the fact that the B^- decay rates depend only weakly on a_2, we obtain, by fitting all 12 branching ratios for which theoretical predictions exist, two possible solutions:

a_1	a_2	χ^2/DoF	prob
0.87 ± 0.08	0.19 ± 0.03	9.2/10	51%
1.03 ± 0.09	-0.20 ± 0.03	6.5/10	77%

Thus, both solutions are equally probable. In the case for D meson decays a relative negative sign for a consistent description within this model is required [3]. The theoretical prediction for the two parameters is $a_1 = 1.1$ and $a_2 = -0.24$ [3], in good agreement with the second solution. This is illustrated in Fig. 11, where the 12 measurements for the two-body B decay channels are compared to the predictions of the Bauer-Stech-Wirbel model, using the second solution.

7 Summary

In conclusion, measurements have been presented of the branching ratios for most of the low-multiplicity B decays involving D, D^*, J/ψ or ψ' mesons. These include first evidence for decay modes involving a D^{*0} or $D_J^{(*)0}$, or through a D^* plus four pions. The mass difference between $\bar{B}^0$ and B^- has been determined to be $(-0.9 \pm 1.2 \pm 0.5)\,\mathrm{MeV/c^2}$. The two-body decay modes are found to be consistent with the model of Bauer, Stech, and Wirbel. Values for the parameters of the model are extracted, with good agreement on the absolute value of the predictions.

Acknowledgements. It is a pleasure to thank U. Djuanda, E. Konrad, E. Michel, and W. Reinsch for their competent technical help in running the experiment and processing the data. We thank Dr. H. Nesemann, B. Sarau, and the DORIS group for the excellent operation of the storage ring. The visiting groups wish to thank the DESY directorate for the support and kind hospitality extended to them.

References

1. Hussain, F., Scadron, M.: Phys. Rev. D30 (1984) 1492
2. Körner, J.G.: Proc. International Symposium on Production and Decay of Heavy Hadrons. Heidelberg 1986
3. Bauer, M., Stech, B., Wirbel, M.: Z. Phys. C – Particles and Fields 34 (1987) 103
4. Savage, M.J., Wise, M.B.: Phys. Rev. D39 (1989) 3346
5. Dobrovolskaya et al.: Phys. Lett. B229 (1989) 293
6. Albrecht, H. et al. (ARGUS Coll.): Phys. Lett. B185 (1987) 218
7. Albrecht, H. et al. (ARGUS Coll.): Phys. Lett. B199 (1987) 451
8. Albrecht, H. et al. (ARGUS Coll.): Phys. Lett. B215 (1988) 424
9. Albrecht, H. et al. (ARGUS Coll.): Nucl. Instrum. Methods A275 (1989) 1
10. Schröder, H.: Proceedings of the Interational Symposium on High Energy Physics. Munich 1988
11. Kubota, Y.: Proceedings of the International Symposium on Heavy Quark Physics. Ithaca NY 1989
12. Harder, G. (ARGUS Coll.): Ph.D. Thesis, University Hamburg, DESY F15-89/01 1989
13. Adler, J. et al. (MARK III Coll.): Phys. Rev. Lett. 60 (1988) 89
14. Adler, J. et al. (MARK III Coll.): Phys. Lett. B208 (1988) 152
15. Hölscher, A. (ARGUS Coll.): Ph.D. Thesis, University Heidelberg 1990
16. Aguilar-Benitez M. et al.: Review of particle properties. Phys. Lett. B204 (1988) 1
17. Anjos, J.C. et al. (Tagged Photon Coll.): Phys. Rev. Lett. 62 (1989) 1717
18. Albrecht, H. et al. (ARGUS Coll.): Phys. Lett. B221 (1989) 422
19. Albrecht, H. et al. (ARGUS Coll.): Phys. Lett. B232 (1989) 398
20. Avery, P. et al. (CLEO Coll.): Phys. Rev. D41 (1990) 774
21. Danilov, M.: Proceedings of the XIV. Int. Symposium on Lepton Photon Interactions. Stanford 1989